of the position parameters are still larger than are normally encountered (Hewat, 1973, 1974) in simple perovskites. Moreover, the R-factor results are not as good as expected, even in the cubic phase where the only structural parameters to refine are B(Pb), B(Zr/Ti) and B_{11} and B_{22} for oxygen.

We thank the Wolfson Foundation for funds supporting this work and AERE (Harwell) and the SRC for facilities on the PANDA diffractometer.

One of us (SAM) acknowledges a grant from the Commonwealth Scholarship Commission in the United Kingdom.

References

ABRAHAMS, S. C., KURTZ, S. K. & JAMIESON, P. B. (1968). *Phys. Rev.* **172**, 551–553.

CLARKE, R. & GLAZER, A. M. (1974). *J. Phys. C*, **7**, 2147–2156.

CLARKE, R. & GLAZER, A. M. (1976*a*). *Ferroelectrics*, **14**, 695–697.

CLARKE, R. & GLAZER, A. M. (1976*b*). *Ferroelectrics*, **12**, 207–209.

CLARKE, R., GLAZER, A. M., AINGER, F. W., APPLEBY, D., POOLE, N. J. & PORTER, S. G. (1976). *Ferroelectrics*, **11**, 359–364.

CLARKE, R. & WHATMORE, R. (1976). *J. Cryst. Growth*, **33**, 29–38.

CLARKE, R., WHATMORE, R. & GLAZER, A. M. (1976). *Ferroelectrics*, **13**, 497–500.

GLAZER, A. M. (1972). *Acta Cryst.* B**28**, 3384–3392.

GLAZER, A. M. (1975). *Acta Cryst.* A**31**, 756–762.

HEWAT, A. W. (1973). *J. Phys. C*, **6**, 2559–2572.

HEWAT, A. W. (1974). *Ferroelectrics*, **6**, 215–218.

JAFFE, B., COOK, W. R. & JAFFE, H. (1971). *Piezoelectric Ceramics*. London: Academic Press.

MEGAW, H. D. & DARLINGTON, C. N. W. (1975). *Acta Cryst.* A**31**, 161–173.

MICHEL, C., MOREAU, J. M., ACHENBACH, G. D., GERSON, R. & JAMES, W. J. (1969). *Solid State Commun.* **1**, 865–868.

RIETVELD, H. M. (1969). *J. Appl. Cryst.* **2**, 65–71.

Acta Cryst. (1978). B**34**, 1065–1070

Powder Profile Refinement of Lead Zirconate Titanate at Several Temperatures. II. Pure $PbTiO_3$

BY A. M. GLAZER AND S. A. MABUD*

Clarendon Laboratory, Parks Road, Oxford OX1 3PU, England

(*Received* 23 *September* 1977; *accepted* 28 *October* 1977)

The structure of pure $PbTiO_3$ has been refined at −183, −115, 25 and 550°C by the Rietveld neutron powder profile method. Positional parameters and temperature factors are given. No evidence was found for the previously reported low-temperature phase transitions.

Introduction

The perovskite $PbTiO_3$ is of interest for several reasons. At room temperature it shows a somewhat higher tetragonal distortion than $BaTiO_3$, with the cation displacements in its polar phase markedly larger. $PbTiO_3$ remains a tetragonal ferroelectric over a wide range of temperature, in contrast to $BaTiO_3$ and similar materials. The ferroelectric-to-paraelectric transition temperature in $PbTiO_3$ is also higher than in any other material possessing the same structure. Moreover, it is regarded as providing an example of a truly classical ferroelectric phase transition (Shirane, Axe, Harada & Remeika, 1970; Burns & Scott, 1973) with a well defined underdamped soft mode.

Industrially, $PbTiO_3$ is an important material because of its potentially high spontaneous polarization (although when pure it appears to have a high conductivity) and because its solid solutions with $PbZrO_3$ (PZT), $BaTiO_3$, $SrTiO_3$ *etc.*, form ceramics with possible technological applications, such as electromechanical transducers, dielectric devices and pyroelectric detectors.

We have grown high-quality single crystals of a suitable size for X-ray and dielectric experiments with a PbO flux. However, crystals large enough for neutron

* On leave from Cavendish Laboratory, Cambridge.

studies were of poor quality and so it was decided to use the neutron powder profile refinement technique (Rietveld, 1969) in order to obtain precise structural information.

The room-temperature phase of $PbTiO_3$ is tetragonal with space group *P4mm*. With the Pb atom at the origin, the positions of all the other atoms in the unit cell are described by three positional parameters, δz_{Ti}, $\delta z_{O(1)}$ and $\delta z_{O(2)}$. The coordinates of all the atoms are then (Fig. 1): Pb at (0,0,0), Ti at $(\frac{1}{2}, \frac{1}{2}, \frac{1}{2} + \delta z_{Ti})$, O(1) at $(\frac{1}{2}, \frac{1}{2}, \delta z_{O(1)})$, O(2) at $(\frac{1}{2}, 0, \frac{1}{2} + \delta z_{O(2)})$ and $(0, \frac{1}{2}, \frac{1}{2} + \delta z_{O(2)})$. The atomic positions were first determined by Shirane, Pepinsky & Frazer (1955, 1956) by both X-ray and neutron diffraction. Their results are: $\delta z_{Ti} = 0{\cdot}040$, $\delta z_{O(1)} = 0{\cdot}112$, $\delta z_{O(2)} = 0{\cdot}112$. With the origin taken so that O(2) is at a height of $\frac{1}{2}c$, the Pb and Ti atoms are shifted in the same direction along **c** by 0·47 and 0·30 Å respectively. In their experiment, the neutron wavelength (1·08 Å) was small and therefore there was considerable overlap of some diffraction lines; at the time, programs enabling the line shapes to be refined (as in the Rietveld program) were not available. Moreover, all the results obtained from the neutron runs were for data collected at a very low angle ($2\theta < 60°$) and therefore the temperature factors refined from them may be unreliable.

In the present experiment, neutron data were collected at several temperatures in an attempt to ascertain the variation of the structural parameters with temperature and to see if there was any sign of the low-temperature phase transition previously reported (Smolenskii, 1951; Kobayashi & Ueda, 1955; Kobayashi, Okamoto & Ueda, 1956; Nomura & Kobayashi, 1958; Ikegami, Ueda & Miyazawa, 1969; Doshi, Glass & Novotny, 1973).

Data collection

Throughout the experiment, $PbTiO_3$ powder of 99·9% purity (Cerac) was used. The quality of the powder was checked by Debye–Scherrer and Guinier photographs, which were compared with those of ceramic material prepared in our laboratory by the usual sintering technique. In addition, the photographs were compared with those of pure single crystals grown from PbO flux.

The neutron diffraction runs were carried out on the PANDA diffractometer at AERE (Harwell) at 25, −115, −183 and at 550°C. The low-temperature data were collected after the specimen had been cooled slowly over a period of 24 h. The measurements were made over a period of 24 h (40 h for the room-temperature run). The low- and room-temperature runs were with the sample enclosed in a vanadium canister; in the 550°C run the sample was in an evacuated silica tube. The wavelength of the incident neutrons was 1·324 Å and the intensities were measured by a bank of nine counters. These were scaled together and summed to increase the signal-to-noise ratio with a set of specially designed computer programs. The method employed has been described in part I of this work (Glazer, Mabud & Clarke, 1978).

Refinement

The ferroelectric properties of $PbTiO_3$ originate in the shifts of the atoms along **c** in the tetragonal unit cell. Because the space group of the tetragonal phase (*P4mm*) is noncentrosymmetric there is considerable uncertainty in the signs of the starting z parameters of Ti, O(1) and O(2). We felt that, rather than bias the outcome of the profile refinement by starting with the previously published structure, different starting models should be tried. We started always by assuming δz_{Ti} to be small and positive (which we may do because it simply defines the positive direction of **c**) and allowing $\delta z_{O(1)}$ and $\delta z_{O(2)}$ to adopt different signs. In addition, some trial models were tried with zeros for the starting parameters. The trial model with $\delta z_{O(1)} = \delta z_{O(2)} = 0$ and with small displacements of Pb and Ti along **c** has the O framework held fixed; we shall refer to it as the rigid-octahedron model. All the other models will be designated by the sign-triplets of the atomic shifts (Table 1). For comparison, the model (000), which corresponds to a structure in which there are no displacements, was also refined. The scattering lengths used in the refinement were: Pb 0·940, Ti −0·340, O $0{\cdot}580 \times 10^{-12}$ cm.

Results from the refinement

During the 25°C run the steel ends of the vanadium canister were inadvertently exposed to the incident neutrons and gave rise to some extra reflections, some of which overlapped those from the sample. These reflections (002, 123, 320 and 004) were therefore omitted from the refinement; for the other runs where

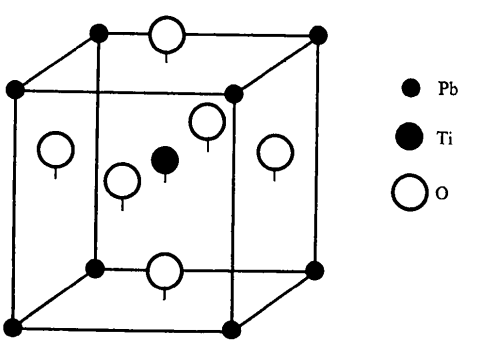

Fig. 1. Diagram of the unit cell of $PbTiO_3$.

Table 1. *Refinement of* $PbTiO_3$ *at room temperature*

Z's denote the z coordinates of the atoms. Figures in brackets denote the corresponding standard deviations.

Trial model assumptions		Starting values of Z_{Ti}	Starting values of $Z_{O(1)}$	Starting values of $Z_{O(2)}$	Refined values of Z_{Ti}	Refined values of $Z_{O(1)}$	Refined values of $Z_{O(2)}$	Refined values of isotropic temperature factors (Å²) B(Pb)	B(Ti)	B[O(1)]	B[O(2)]	R factors (%) R_{nuc}	R_{prof}	R_w	R_{exp}	Number of parameters refined
(+++)	$B_{O(1)} = B_{O(2)}$	0·51	0·08	0·60	0·539 (0·002)	0·114 (0·002)	0·617 (0·002)	0·691 (0·086)	0·032 (0·166)	0·441 (0·064)	0·441 (0·064)	4·38	10·21	12·85	2·96	15
(+++)	$B_{O(1)} \neq B_{O(2)}$	0·51	0·08	0·60	0·539 (0·002)	0·114 (0·002)	0·617 (0·002)	0·706 (0·089)	0·061 (0·170)	0·352 (0·117)	0·477 (0·075)	4·35	10·19	12·83	2·96	16
(+++)	$B_{O(1)} = B_{O(2)}$	0·56	0·14	0·64	0·539 (0·002)	0·114 (0·002)	0·617 (0·002)	0·690 (0·086)	0·029 (0·166)	0·441 (0·064)	0·441 (0·064)	4·37	10·21	12·85	2·96	15
(+++)	$B_{O(1)} \neq B_{O(2)}$	0·56	0·14	0·64	0·539 (0·002)	0·114 (0·002)	0·617 (0·002)	0·706 (0·089)	0·060 (0·170)	0·351 (0·117)	0·477 (0·075)	4·35	10·19	12·83	2·96	16
(++0)	$B_{O(1)} \neq B_{O(2)}$	0·54	0·09	—	0·550 (0·003)	0·129 (0·002)	—	1·753 (0·118)	0·643 (0·242)	−0·724 (0·101)	0·383 (0·091)	9·74	14·21	17·10	2·96	15
(+−0)	$B_{O(1)} \neq B_{O(2)}$	0·54	−0·09	—	0·451 (0·003)	−0·129 (0·002)	—	1·744 (0·121)	0·688 (0·254)	−0·738 (0·102)	0·405 (0·097)	9·58	14·23	17·15	2·96	15
(+−+)	$B_{O(1)} \neq B_{O(2)}$	0·54	−0·09	0·60	0·462 (0·002)	−0·112 (0·002)	0·553 (0·002)	0·890 (0·110)	0·268 (0·196)	−0·040 (0·119)	0·534 (0·083)	6·31	11·35	13·47	2·96	16
(++−)	$B_{O(1)} \neq B_{O(2)}$	0·551	0·09	0·40	0·538 (0·002)	0·112 (0·002)	0·467 (0·002)	0·885 (0·110)	0·263 (0·196)	0·035 (0·120)	0·534 (0·083)	6·29	11·34	13·47	2·96	16
(+−−)	$B_{O(1)} \neq B_{O(2)}$	0·551	−0·09	0·40	0·461 (0·002)	−0·114 (0·002)	0·383 (0·002)	0·701 (0·088)	0·065 (0·170)	0·347 (0·117)	0·476 (0·075)	4·36	10·20	12·84	2·96	16
(0+−)	$B_{O(1)} \neq B_{O(2)}$	—	0·11	0·45	—	0·103 (0·002)	0·461 (0·002)	0·403 (0·104)	1·372 (0·246)	0·233 (0·171)	1·001 (0·113)	7·91	13·22	15·74	2·96	15
(000)	$B_{O(1)} \neq B_{O(2)}$	—	—	—	—	—	—	−0·211 (0·118)	1·209 (0·512)	3·339 (0·423)	4·228 (0·336)	29·80	32·73	36·64	2·96	13
Rigid-octahedron model		0·60	0·10	0·60	0·539 (0·002)	0·116 (0·002)	0·616 (0·002)	0·691 (0·086)	0·071 (0·166)	0·440 (0·064)	0·440 (0·064)	4·65	10·23	12·89	2·96	14
Literature results					0·540	0·112	0·612		Overall B = 0·30							

Table 2. *Summary of parameters refined at all temperatures* (Pb *at origin*)

	−183°C	−115°C	25°C	550°C
Isotropic temperature factor refinement				
δz_{Ti}(Å)	0·167	0·171	0·162	0
$\delta z_{O(1)}$(Å)	0·492	0·479	0·473	0
$\delta z_{O(2)}$(Å)	0·505	0·504	0·486	0
B(Pb)	0·378 (100)	0·757 (84)	0·706 (89)	2·711 (167)
B(Ti)	0·284 (215)	0·364 (187)	0·060 (170)	0·694 (225)
B[O(1)]	0·670 (140)	0·713 (123)	0·351 (117)	1·549 (102)
B[O(2)]	0·498 (98)	0·862 (85)	0·477 (75)	B[O(1)]
R_{nuc}	5·22	5·90	4·35	3·10
R_{prof}	12·47	12·21	10·19	12·07
R_w	15·20	15·87	12·83	16·57
Anisotropic temperature factor refinement				
B_{11}(Pb)†	0·072 (216)	0·751 (151)	0·554 (144)	2·710 (165)
B_{33}(Pb)	0·256 (253)	0·805 (200)	0·864 (187)	B_{11}(Pb)
B_{11}(Ti)	0·189 (537)	0·092 (283)	−0·128 (228)	0·715 (229)
B_{33}(Ti)	−0·084 (913)	0·700 (657)	0·710 (595)	B_{11}(Ti)
B_{11}[O(1)]	0·375 (324)	0·832 (204)	0·786 (235)	0·881 (316)
B_{33}[O(1)]	1·626 (444)	1·126 (288)	0·412 (248)	2·992 (795)
B_{11}[O(2)]	0·963 (285)	0·669 (226)	0·623 (271)	B_{11}[O(1)]
B_{22}[O(2)]	0·511 (316)	0·304 (269)	−0·331 (294)	B_{33}[O(1)]
B_{33}[O(2)]	1·138 (445)	1·312 (238)	0·922 (209)	B_{11}[O(1)]
R_{nuc}	4·86	6·08	4·53	2·88
R_{prof}	11·81	12·18	10·01	11·90
R_w	14·78	15·84	12·61	16·43
a(Å)	3·895	3·899	3·905	3·970
c(Å)	4·171	4·167	4·156	

† Refinement of anisotropic temperature factors did not alter appreciably the values of atomic displacements. $B_{11} = 4\beta_{11}/(a^*)^2$, $B_{22} = 4\beta_{22}/(b^*)^2$ and $B_{33} = 4\beta_{33}/(c^*)^2$, where the temperature factor is given by $\exp[-(\beta_{11}h^2 + \beta_{22}k^2 + \beta_{33}l^2 + 2\beta_{12}hk + 2\beta_{23}kl + 2\beta_{31}lh)]$.

this difficulty did not arise the refinement was sufficiently similar to say that the omission of these reflections did not seriously affect the refinement results.

Table 1 lists the results for the refinement of the various models with the 25 °C data; here, isotropic temperature factors were refined as well as positional parameters. The R factors are defined by

$$R_{\text{nuc}} = 100\,\Sigma\,|I(\text{obs.}) - SI(\text{calc.})|/\Sigma\, I(\text{obs.}),$$

$$R_{\text{prof}} = 100\,\Sigma\,|y_i(\text{obs.}) - Sy_i(\text{calc.})|/\Sigma\,|y_i(\text{obs.})|,$$

$$R_{\text{exp}} = 100\sqrt{\{(N-P)/\Sigma\, w[y(\text{obs.})]^2\}},$$

and

$$R_w = 100\sqrt{\{\Sigma\, w[y(\text{obs.}) - Sy(\text{calc.})]^2/\Sigma\, w[y(\text{obs.})]^2\}},$$

where I(obs.), I(calc.) = observed and calculated integrated intensity of a reflection, y_i(obs.), y_i(calc.) = observed and calculated intensity data point, w = weighting factor, N = number of observations y_i, P = number of parameters, and S = scale factor. It can be seen that model (+−−) refined to the model (−−−) which is the same as (+++). Also the model (000), which attempts to simulate a cubic structure refined with the observed intensities, shows poor agreement.

To decide between these various models, significance tests (Hamilton, 1965) were applied to the weighted R factors (R_w) obtained. As the value of R_w was lowest for the (+++) model we took it to be the 'unrestrained' model and compared it with the others. This led to the conclusion that the (+++) model was certainly more likely (99·5% significance) than (++−). On the other hand, it is not possible to decide between (+++) and the rigid-octahedron model. Note the close similarity of all the parameters in both models to the literature values (Table 1).

It can be seen that the B(Ti) is unusually small at room temperature; for this reason, anisotropic temperature factor refinement was also tried. The results are listed in Table 2. The most noticeable features are the extreme anisotropies of the thermal ellipsoids for Ti.

Table 2 also lists the results for the (+++) model at all the temperatures for which data were collected and Fig. 2 shows the observed and calculated intensity profiles.

Discussion of results of refinement

$PbTiO_3$ retains its tetragonal structure down to −183 °C; no sign was found of the previously reported low-temperature phase transitions, despite the low rate of cooling used. This should be contrasted with the isostructural materials, $BaTiO_3$ and $KNbO_3$, where a sequence of phase transitions occurs on cooling: cubic → tetragonal → orthorhombic → rhombohedral. Fig. 3 shows the labelling of the atoms and Table 3 gives the bond lengths and angles. The Ti–O(1) length (No. 1) is

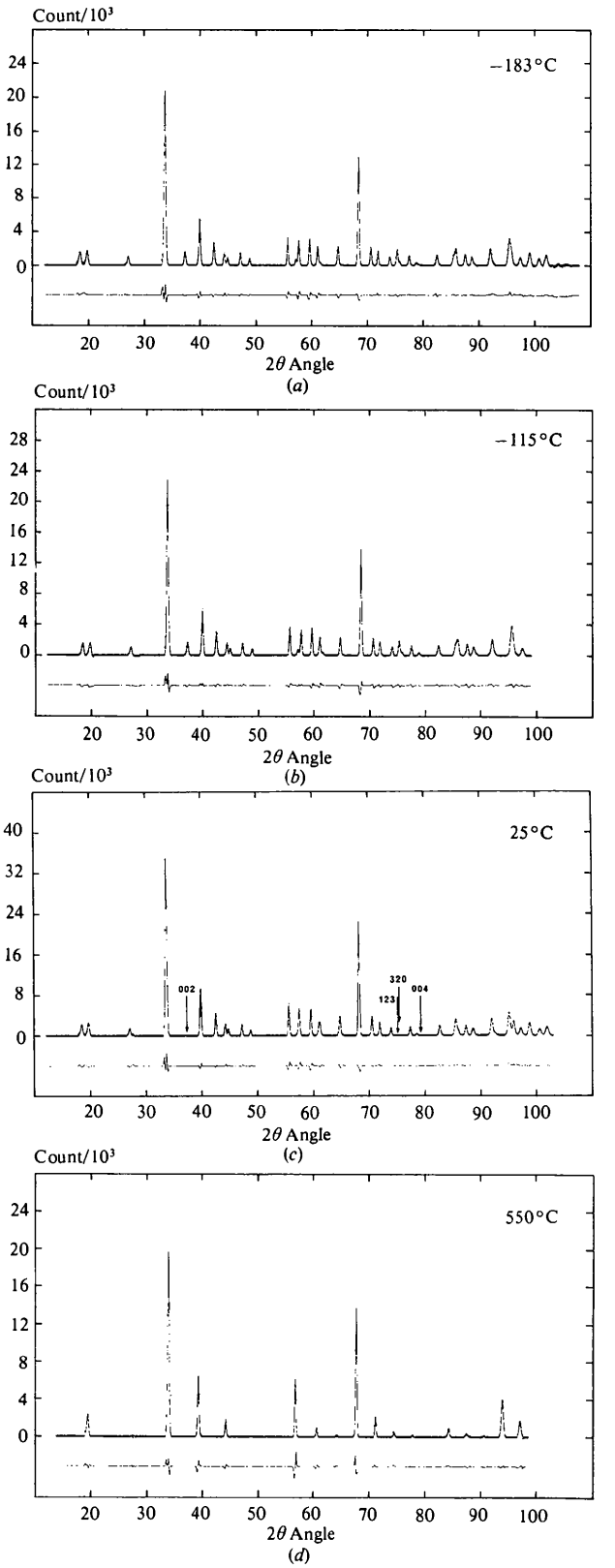

Fig. 2. Observed and calculated intensity profiles for each run. Arrows indicate reflections omitted from refinement. The lower trace shows y(obs.) − y(calc.).

Table 3. *Bond lengths* (Å) *and angles* (°) *for the rigid-octahedron model*

		−183 °C	−115 °C	25 °C	550 °C (cubic phase)
(1)	Ti–O(1)	1·75	1·76	1·76	1·99
(2)	Ti–O(1)	2·42	2·41	2·40	
(3)	Ti–O(2)	1·98	1·98	1·98	
(4)	O(1)–O(2)	2·85	2·85	2·85	2·81
(5)	O(2)–O(2)	2·75	2·76	2·76	
(6)	Pb–O(1)	2·83	2·80	2·80	2·81
(7)	Pb–O(2)	2·51	2·51	2·52	
(8)	Pb–O(2)	3·24	3·23	3·21	
(7)–(7′)	O(2)–Pb–O(2)	101·8	101·8	101·5	90·0
(7)–(8)	O(2)–Pb–O(2)	92·1	92·1	91·9	
(8)–(8′)	O(2)–Pb–O(2)	73·9	74·1	74·7	

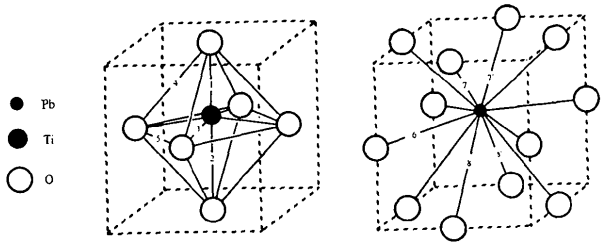

Fig. 3. Labelling of atoms for Table 3.

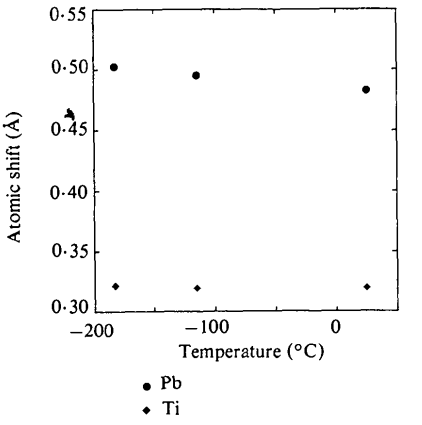

Fig. 4. Plot of Pb and Ti displacements in Å along [001] as a function of temperature, with the origin chosen on the O(2) plane, assuming the O octahedra to be rigid.

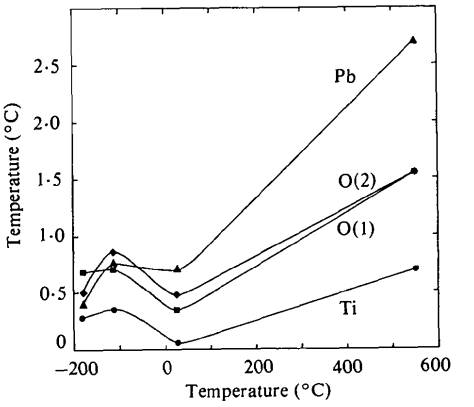

Fig. 5. Plot of isotropic temperature factors as a function of temperature. Error bars have been omitted for clarity.

considerably smaller at all temperatures than the sum of the Goldschmidt radii of Ti^{4+} and O^{2-}. [Similarly for the Pb–O(2) length (No. 7).]. This has been explained by Megaw (1954) by allowing changes in the ionic characters of the relevant atoms. It is also clear from Table 3 that, despite the large range of temperatures used, the bond lengths and angles are remarkably constant, suggesting that the structure is very rigid.

However, the *c/a* ratio increases as the temperature is lowered and this gives rise to an increase in the displacements of Pb and Ti relative to the O octahedron. In Fig. 4 these shifts are plotted *versus* temperature. The shift of Pb is more than 1·5 times that of Ti throughout the entire temperature range studied. This is to be contrasted with $BaTiO_3$ where the Ti displacement is twice that of Ba.

The Ti shift in Fig. 4 can be used to estimate the spontaneous polarization from the relationship $P_s = k\delta z$ (Abrahams, Kurtz & Jamieson, 1968). With $k = 2{\cdot}90 \pm 0{\cdot}04$ C m^{-2} Å^{-1}, derived in part I of this work, $P_s = 0{\cdot}92$ C m^{-2} at 25 °C, a value which is close to the previously measured value of 0·75 C m^{-2} (Gavrilyachenko, Spinko, Martynenko & Fesenko, 1970), but rather larger than the value of 0·57 C m^{-2} given by Remeika & Glass (1970). The constancy of Ti displacements with decreasing temperature indicates that P_s will not alter as the temperature is lowered; as yet, no measurements have been made of P_s *versus* temperature over this range.

Finally, in Fig. 5 the isotropic temperature factors are plotted as a function of temperature. Although the results are rather rough they do seem to indicate some interesting behaviour. From room temperature to 550 °C they all increase, as expected. On the other hand, the low-temperature results suggest a small maximum at around −100 °C. It is possible that this indicates the proximity of a transition to another phase near −100 °C which, in our case, according to single-crystal studies at low temperature (unpublished) never actually took place. Further work is needed before anything definite can be said about this effect.

We are grateful to the Wolfson Foundation for funds supporting this research. One of us (SAM) acknow-

ledges a grant from the Commonwealth Scholarship Commission. We are indebted to R. Clarke for useful discussion.

References

ABRAHAMS, S. C., KURTZ, S. K. & JAMIESON, P. B. (1968). *Phys. Rev.* **172**, 551–553.
BURNS, G. & SCOTT, B. A. (1973). *Phys. Rev. B*, **7**, 3088–3101.
DOSHI, P., GLASS, J. & NOVOTNY, M. (1973). *Phys. Rev. B*, **7**, 4260–4263.
GAVRILYACHENKO, V. G., SPINKO, R. O., MARTYNENKO, M. A. & FESENKO, E. G. (1970). *Sov. Phys. Solid State*, **12**, 1203–1204.
GLAZER, A. M., MABUD, S. A. & CLARKE, R. (1978). *Acta Cryst.* B**34**, 1060–1065.
HAMILTON, W. C. (1965). *Acta Cryst.* **18**, 502–510.
IKEGAMI, S., UEDA, I. & MIYAZAWA, T. (1969). *J. Phys. Soc. Jpn*, **26**, 1324.
KOBAYASHI, J., OKAMOTO, S. & UEDA, R. (1956). *Phys. Rev.* **103**, 830.
KOBAYASHI, J. & UEDA, R. (1955). *Phys. Rev.* **99**, 1900–1901.
MEGAW, H. D. (1954). *Acta Cryst.* **7**, 187–194.
NOMURA, S. & KOBAYASHI, J. (1958). *J. Phys. Soc. Jpn*, **13**, 114–115.
REMEIKA, J. P. & GLASS, A. M. (1970). *Mater. Res. Bull.* **5**, 37–46.
RIETVELD, H. M. (1969). *J. Appl. Cryst.* **2**, 65–71.
SHIRANE, G., AXE, J. D., HARADA, J. & REMEIKA, J. P. (1970). *Phys. Rev. B*, **2**, 155–159.
SHIRANE, G., PEPINSKY, R. & FRAZER, B. C. (1955). *Phys. Rev.* **97**, 1179–1180.
SHIRANE, G., PEPINSKY, R. & FRAZER, B. C. (1956). *Acta Cryst.* **9**, 131–140.
SMOLENSKII, G. A. (1951). *Zh. Tekh. Fiz.* **21**, 1045–1049.

Acta Cryst. (1978). B**34**, 1070–1074

$BaZrF_6$ α: Une Structure à Anion Complexe $[Zr_2F_{12}]^{4-}$

PAR JEAN-PAUL LAVAL, RENÉE PAPIERNIK ET BERNARD FRIT

Laboratoire de Chimie Minérale Structurale, UER des Sciences Exactes et Naturelles, 123 *rue Albert Thomas,* 87060 *Limoges, France*

(*Reçu le* 28 *septembre* 1977, *accepté le* 26 *octobre* 1977)

α-$BaZrF_6$ is monoclinic, with $a = 6{\cdot}493$ (2), $b = 9{\cdot}530$ (3), $c = 9{\cdot}203$ (3) Å, $\beta = 127{\cdot}09$ (7)°, space group $P2_1/c$. The structure was solved by three-dimensional Patterson and Fourier techniques and refined by least-squares procedures to a conventional $R = 0{\cdot}028$, for 1021 independent reflexions recorded on an automatic diffractometer. The structure is built up of unique $[Zr_2F_{12}]^{4-}$ complex anions resulting from the association of two monocapped trigonal prisms sharing an edge, linked by Ba^{2+} cations.

Dans une publication antérieure (Laval, Mercurio-Lavaud & Gaudreau, 1974) nous annoncions la préparation et l'étude structurale de quatre fluorozirconates de formule générale $M^{II}ZrF_6$ (M = Sr, Ba, Pb et Eu), les deux derniers étant inédits. Trois d'entre eux, les fluorozirconates de strontium(II), baryum(II) et europium(II) se révélaient dimorphes et nous montrions que le fluorozirconate de plomb ainsi que les variétés basse température de $SrZrF_6$ et $EuZrF_6$ et haute température de $BaZrF_6$ étaient isotypes, cristallisant dans le système orthorhombique avec pour groupe d'espace *Cmma* ou *Abm*2. L'étude structurale complète, sur monocristal de $PbZrF_6$, permettait de montrer que leur structure cristalline était du type $RbPaF_6$. Ces résultats ont été récemment confirmés pour l'essentiel par Mehlhorn & Hoppe (1976) qui, s'ils vérifient bien l'isotypie et le type structural des quatre composés cités, ne signalent par contre pas l'existence du polymorphisme de $SrZrF_6$, $BaZrF_6$ et $EuZrF_6$.

Etude préliminaire; constantes radiocristallographiques de $BaZrF_6$ α

Par ATD, la transition réversible $\alpha \rightleftharpoons \beta$ a pu être située à 544 ± 5 °C, la fusion congruente intervenant à 574 ± 5 °C.

Un monocristal de forme quasi-sphérique et de rayon $R \simeq 0{,}08$ mm a été isolé d'une préparation de composition $ZrF_4.BaF_2$, portée à fusion et refroidie lentement jusqu'à 450 °C, puis maintenue quatre jours à cette température. Le spectre X de poudre de cette